

## DAΦNE Beam-Test Facility (BTF)

B. Buonomo, C. Di Giulio (Art. 23), L. G. Foggetta (Art. 23),  
P. Valente (Resp., Ass.)

M. Belli (Tecn.), R. Ceccarelli (Tecn.), A. Cecchinelli (Tecn.), R. Clementi (Tecn.),  
G. Piermarini (Tecn.), S. Strabioli (Tecn.), L. A. Rossi (Tecn.), R. Zarlunga (Tecn.)

F. Casarin (Amm.), M. R. Ferrazza (Amm.), M. Giabbai (Amm.)

### Introduction

Test beam and irradiation facilities are key enabling infrastructures for research in HEP and astroparticles. In the last 12 years the Beam-Test Facility (BTF) of the DAΦNE accelerator complex has gained an important role in the European infrastructures devoted to the development and testing of particle detectors. Electrons or positrons can be extracted (see Fig. 1) before the injection into the damping ring, on a bunch-by-bunch basis, by means of a pulsed dipole (DHPTB101); then the beam is driven to the BTF dedicated transfer line, where a system composed by a target (TGTTB01) plus a dipole (DHSTB01) and collimating slits (SLTTB02 upstream and SLTTB03-04 downstream), can attenuate and select the momentum of secondary particles in narrow ( $< 1\%$ ) band. The secondary beam is then driven to the experimental hall and focussed by means of the QUATB01-04 quadrupoles. The final  $45^\circ$  bending is performed by the DHSTB02 dipole. Horizontal and vertical correctors (CHVTB01-02) provide fine adjustment of the trajectory.

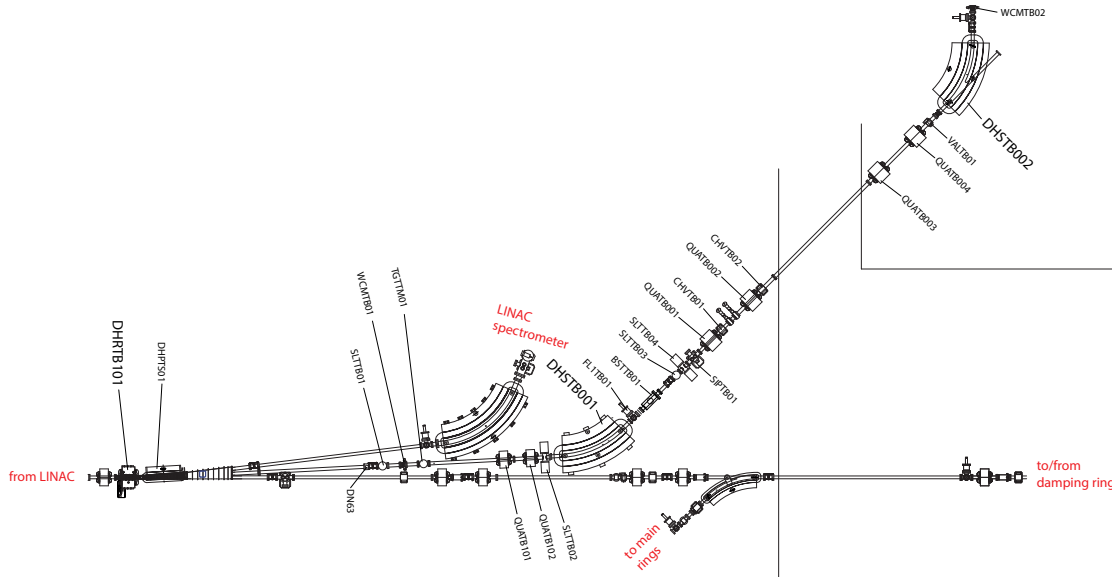


Figure 1: *Layout of BTF line elements.*

The facility can provide run-time tuneable electrons and positrons beams in a defined range of different parameters: energy (up to 750 MeV for  $e^-$  and 550 MeV for  $e^+$ ), charge (from the “single particle” regime up to  $10^{10}$  particles/bunch) and pulse length (1.4–40 ns). The bunch delivering rate is depending on the DAΦNE injections (up to 49 Hz). The electron beam spot and divergence

can be adjusted, down to sub-mm sizes and approximately 2 mrad in air. The BTF has to balance the beam-time and staff effort between different needs:

- running the facility for the benefit of the largest possible users range (Sec. 1);
- improving the flexibility and reliability, constantly improving the diagnostics and tools, both hardware and software (Sec. 2);
- preparing for the future, planning, designing and performing the upgrades (Sec. 3), needed to enlarge the use and application range of the BTF and LINAC <sup>1)</sup>.

## 1 The BTF running with users

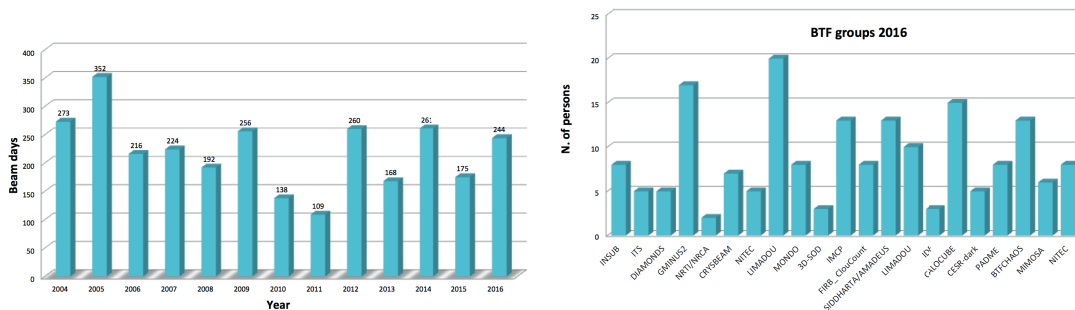


Figure 2: Summary of BTF delivered beam-days since 2004 (left) and number of users in year 2016 shifts (right).

In Fig. 2 the summary of users access to BTF is shown: the number of beam-days available to users in 2015 was limited to 175 due to the time needed for the dismantling and mounting in the new configuration the shielding blocks of the experimental hall shielding (see Sec. 3), while it was well above the average ( $\approx 220$ ) in year 2016, when 21 teams were hosted for a grand total of 189 users (with double counting).

## 2 The BTF diagnostics, monitoring and controls improvements

Proficient running at the BTF is possible thanks to a variety of services made available to the users: power supply, networking, gas system, DAQ and beam diagnostics, vacuum and cryogenics, alignment, and magnetic fields <sup>2)</sup>.

In characterizing and calibrating high-energy physics particle detectors one very common requirement is to have a charged particle beam as better spatially defined as possible, both in the transverse size and direction (angular divergence). Rich diagnostics allows controlling and monitoring the beam main parameters: calorimeters, Silicon pixel, GEM gas detectors in the low and intermediate intensity regime, and fluorescent flags and integrating current toroid at high intensity <sup>3)</sup>. The improved resolution achieved by means of FitPIX (by ADVACAM) Silicon pixel detector based on the Timepix chip, allowed to precisely characterize the beam spot as a function of the selected beam energy and of the BTF line optics setting. The main limitation for achieving a "pencil" beam is mainly given by the Coulomb multiple scattering (MS), as soon as electrons leave the vacuum pipe where they are transported and focussed down to the BTF hall.

There are two contributions to the MS that cannot be easily removed: the Beryllium, 0.5 mm thick window at the exit of the pipe, and the air in between the exit window and the device under test. The practical formula for the MS angular spread on particles of charge  $z$  on a material of thickness  $x$  and radiation length  $x_0$

$$\theta_{\text{MS}} \simeq \frac{13.6}{\beta c p} z \sqrt{\frac{x}{x_0}}$$

indicates that the widening of the beam is inversely proportional to the particle momentum  $p$ . This has been very well reproduced during the LIMADOU satellite payload test and calibration runs (two weeks in year 2016), for which electron beams of energy as low as 30 MeV have been selected, as shown in Fig. 3.

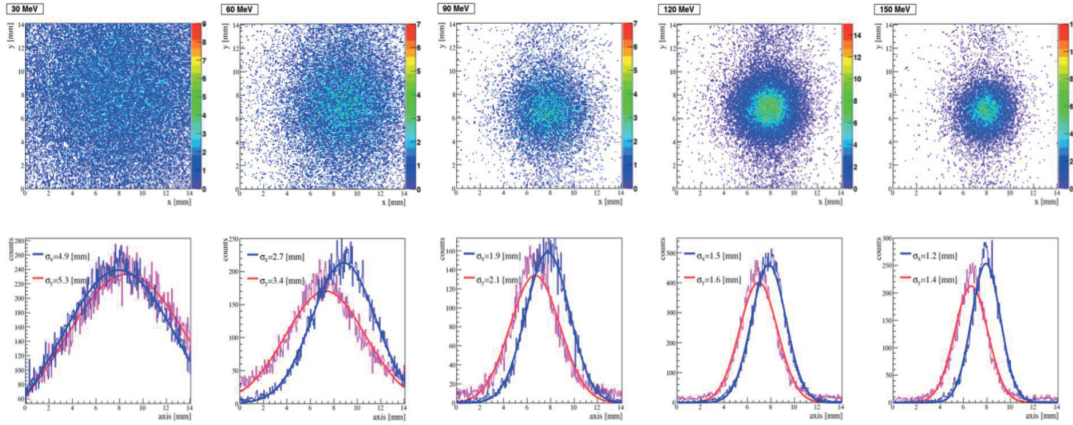


Figure 3: *Low energy beam spot optimization for the LIMADOU satellite payload test; electron beam energy ranging from 30 to 150 MeV (from left to right in 30 MeV steps): 2D transverse distribution (top row) and  $x, y$  profile histograms (bottom row) obtained from FitPIX detector.*

The MS effect due to the 0.5 mm Beryllium can be estimated to be 1.1 mrad at 450 MeV. The contribution of the beam divergence before crossing the beam-pipe window can thus be estimated to be  $< 1$  mrad, since a beam spot of the order of  $\sigma_{x,y} \approx 0.5$  mm is achieved at a distance of 36 cm, as shown in Fig. 4 .

### 3 The BTF upgrades

An important upgrade program of the facility is under way, along different lines <sup>4)</sup>:

- consolidation of the LINAC infrastructure, in order to guarantee a stable operation in the longer term <sup>5)</sup>;
- optimization of the operational parameters for irradiation and high-intensity test. For this purpose an improvement of the BTF hall shielding has also been performed;
- increase of the beam pulse length (limited to 10 ns during DAΦNE injection and to 40 ns by the existing gun-pulsing system) in order to get higher beam intensity while keeping constant particle density <sup>6)</sup>;

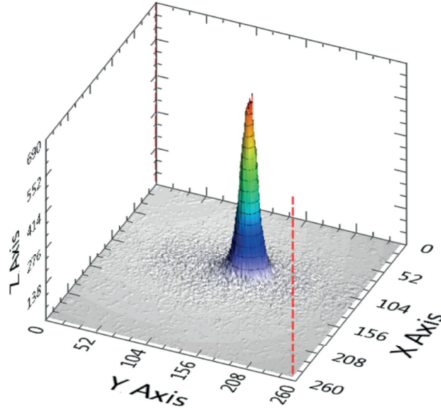


Figure 4: *The 2D transverse distribution obtained from FitPIX detector for a 450 MeV electron beam.*

- doubling of the BTF beam-lines, in order to cope with the significant increase of users due to the growing range of applications.

An energy upgrade of the LINAC, in order to increase the facility capability (especially for the almost unique extracted positron beam), has also been proposed: by adding four more accelerating sections in the last  $\approx 15$  m of drift space at the end of the LINAC should allow reaching 1 GeV with a relatively low cost.

In order to reach an energy as high as 750 MeV in  $\approx 60$  m of the S-band LINAC, the accelerating field is increased thanks to the compression of the radio-frequency (RF) produced by the four klystrons by the SLED devices: the coupled resonant cavities accumulate the otherwise flat RF power (over an interval of  $4.5\mu\text{s}$ ), until a  $180^\circ$  phase inversion of the input from the klystron produces a sharp peak in the accelerating field. The maximum field is thus reached over a flat top of few tens of ns, increasing the accelerating gradient up to 17 MV/m in the standard sections and 26 MV/m in the capture section. This is generally not an issue when producing 10 ns pulses for injection into the DAΦNE rings, but in order to accelerate much longer trains of 2856 MHz micro-bunches the effect of decreasing voltage felt by the tail of the pulse with respect of the head should be compensated.

After having upgraded the gun pulsing system, previously limited to 40 ns, with a new supply capable of generating up to  $5\mu$  high-voltage waveforms, longer pulses can be produced. In order to accelerate them the LINAC configuration has to be changed in a number of ways:

- increasing the phase acceptance at the output of the buncher cavities (“packing” electrons emitted by the gun in the time structure of the RF);
- increasing the field of the Helmholtz coils in the buncher region in order to get a better focussing of the longer pulses;
- increasing the power in the first accelerating section, in order to recover the lower acceptance;
- changing the timing of the electron gun with respect to the RF, in order to compensate for the decrease of field at the end of the pulse;
- compensating for the lower energy gain by adjusting the RF phases and the power in the following sections.

In Fig. 5 the current monitor signals in four different spots of the LINAC are shown with this optimized configuration: at the exit of the electron gun (yellow trace), after the first five accelerator sections and immediately upstream of the positron converter (cyan,  $E_e \approx 200$  MeV), after the first two positron sections and upstream of the last LINAC sections (purple), and at the end of the LINAC (green). Pulses as long as 280 ns have been successfully accelerated up to 450 MeV, with a  $\approx 2\%$  energy spread, so that further optimization and tuning are needed.

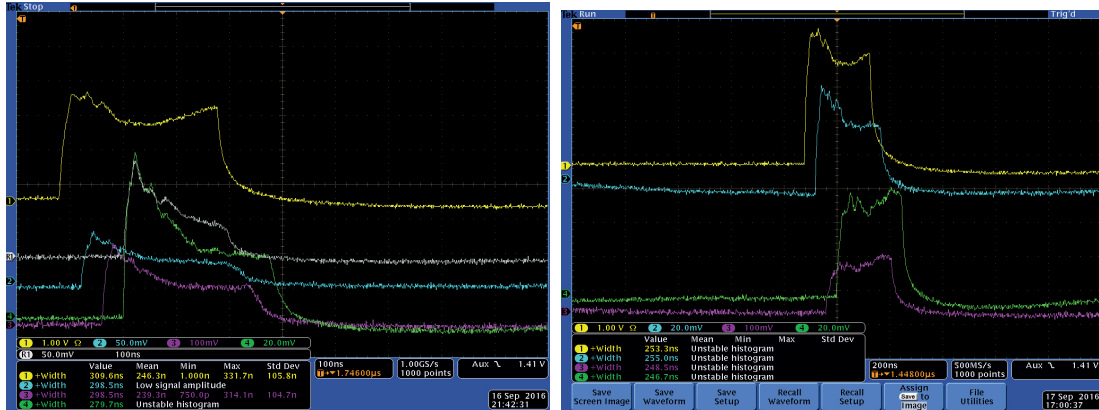


Figure 5: *Electrons produced by the new pulsing system (yellow traces) and accelerated by the DAΦNE LINAC in pulses longer than the standard 10 ns: before any optimization a clear decrease of the intensity along the pulse length of 280 ns is visible (left, green trace is the end of the LINAC); after a first tuning slightly shorter pulses are obtained with a more flat profile (right).*

In Fig. 6 the BTF hall before and after the re-arrangement of shielding blocks and the covering of the experimental area with 50 cm thick concrete bins is shown.



Figure 6: *Shielding blocks in the BTF experimental hall: before (left) and after (right) the re-arrangement and realization of the coverage.*

### 3.1 LINAC consolidation and beam pulse extension

An extensive maintenance program has been performed on all the LINAC components, in particular on the four RF power stations. Several components such as filter capacitors, thyratrons and high power pulse discrete elements have been replaced, and a newly designed RF driver system has been installed, in order to achieve a better stability of the delivered power. In critical parts,

like waveguides downstream the SLEDs, additional pumps with higher pumping speed have been added, in order to reduce discharge occurrences. All the ceramic windows, placed downstream the klystron ones to decouple the LINAC vacuum, have been substituted. The LINAC control system has been revised in order to be compatible with the new network infrastructure. Also the control of the cooling has been upgraded to a new PLC-based system, together with a revision of the water ducts, flux-meters and water pumping system of the primary cooling system (at 30° C).

A new electron gun system has been also developed and put into operation, with the main purpose of accelerating longer electron and positron macro-bunches: the existing power supply could deliver HV pulses in the range 1.5 – 40 ns, while the requirement for some applications, like for instance the PADME dark photon experiment, is of low-density longer beam pulses (up to several hundreds of ns).

### 3.2 Beam line splitting

The present BTF configuration practically makes available only a useful beam exit (parallel to the long side of the BTF experimental hall). The useful experimental area, downstream of the DHSTB02 45° dipole, is presently used for the beam-tests, and is equipped with the remotely controlled trolley, FitPIX and GEM diagnostics, scintillator hodoscope, and so on. The exit at the end of the straight beam line (receiving beam when DHSTB02 is off), which points towards the lateral wall of the hall, is currently used for high-intensity electron runs, typically with the neutron production target, and as photon exit with the tagged photon source

The idea for the new layout is schematically shown in Fig. 7: a beam-splitting magnet (the 15° dipole DP01), wrapped around a double-exit pipe, can drive beam pulses from the upstream BTF beam-line alternatively to the two new lines. This dipole can be connected to a pulsed power supply for a fast switch between the two lines.

In order to have sufficient space and to allow bending the beam towards the former control room, it has to be placed as close as possible to the entry point of the BTF vacuum-pipe in the present experimental hall. One line will be turned by 45° using the existing DHSTB02, in a configuration very similar to the existing BTF line. The available space will be only slightly reduced in the transverse direction with respect to the beam to a useful surface of about  $3 \times 6 \text{ m}^2$ .

The second, new line, will be further bent (by two additional 45° dipoles) in order to enter the former control room close to the intersection of the two perpendicular walls of the control room. A hole in the wall separating the two rooms should be realized. Since the entire area has a kind of L-shape, an additional angle will be needed in order to complete the 90° turn, thus directing the beam parallel to the long side of the second hall, by means of a last dipole (DC01).

In order to preserve the beam quality, to this basic configuration quadrupoles and correctors have been added, after a careful optimization of the optics of the two lines with MAD-X and with G4beamline codes.

In order to use the new experimental area, the present control room should have to be dismantled and moved in some other place, and an adequate shielding should be foreseen. Taking into account that the new room has to be shielded with concrete blocks as the existing one, and considering a depth of 1 m, the useful surface in this new hall will be of about  $3 \times 5 \text{ m}^2$ . Preliminary calculations show that this kind of shielding, covered by a concrete beam roof, will allow keeping the dose outside of the restricted area below the required level of 0.6 mSv/year (0.1  $\mu\text{Sv/h}$  for 6000 hours of operation).

A new control room for the BTF has been already prepared, refurbishing and adapting the control room in the past used for the ADONE accelerator before and for the FINUDA experiment, after the start of the DAΦNE project. This new control room, shown in Fig. 8, is on the upper floor with respect to the BTF area, close to the main DAΦNE main control room.



Figure 7: The new BTF layout with two beam-lines and two experimental areas.



Figure 8: The new BTF control room.

## 4 Irradiation

The main requirements for running the BTF as an electron irradiation facility are the following:

- High fluence of electrons of well defined energy (10%) over a wide range: down to few tens of MeV and up to the GeV range;
- Uniformity of irradiation over a  $\mathcal{O}(\text{cm}^2)$  surface within 10%;
- Determination of the dose with an uncertainty better than 10%.

The present BTF beam quality is adequate, provided that a better and calibrated fluence and uniformity diagnostics is provided to the irradiation users, as required, for instance, by ESA ESCC (European Space Component Coordination) guidelines. Preliminary studies of the defocused beam, in order to control the uniformity at the required level, demonstrate that BTF can be qualified quickly as an irradiation facility, suitable for space qualification. Preliminary contacts with the Italian Space Agency (ASI) have been established, in order to both qualify the BTF as a facility recognized by ESA, and to include it in a network of Italian irradiation facilities for space (ASIF). With similar purposes, BTF is also included in the NASA-SSERVI solar system exploration program, in collaboration with the American space agency and the Frascati spatial qualification laboratory (SCF-LAB).

## 5 AIDA-2020

The BTF is part of the Horizon 2020 project AIDA-2020, GA no. 654168, in particular in the Work-Package 15 the task 15.4 is aimed at achieving “Improvements of the test beam infrastructure at INFN-LNF”.

## 6 Education and outreach

Several activities have been carried on in the field of education and outreach:

1. EDIT 2015 school, October 2015;
2. Beamline for Schools (INFN branch);
3. Incontri di Fisica;
4. Visiting students from Insubria University.

## 7 List of Papers by BTF Users in 2015-2016

1. G. Piperno *et al.*, “The PADME experiment at Laboratori Nazionali di Frascati”, arXiv:1608.00036 [physics.ins-det].
2. S. Fiore *et al.*, “The PADME experiment at INFN LNF”, J. Phys. Conf. Ser. **770** (2016) no.1, 012039. doi:10.1088/1742-6596/770/1/012039
3. A. Aloisio *et al.*, “A pure CsI calorimeter for the Belle II experiment at SuperKEKB”, Nucl. Instrum. Meth. A **824** (2016) 704. doi:10.1016/j.nima.2015.11.045
4. R. Becker *et al.*, “Test beam results with a sampling calorimeter of cerium fluoride scintillating crystals and tungsten absorber plates for calorimetry at the HL-LHC”, Nucl. Instrum. Meth. A **824** (2016) 681. doi:10.1016/j.nima.2015.09.052

5. Becker:2015rca R. Becker *et al.*, “Beam test results for a tungsten-cerium fluoride sampling calorimeter with wavelength-shifting fiber readout,” JINST **10** (2015) no.07, P07002. doi:10.1088/1748-0221/10/07/P07002
6. A. Antonelli, F. Gonnella, V. Kozhuharov, M. Moulson, M. Raggi and T. Spadaro, “Study of the performance of the NA62 Small-Angle Calorimeter at the DAΦNE Linac”, arXiv:1610.03827 [physics.ins-det].
7. A. Anastasi *et al.*, “Electron beam test of key elements of the laser-based calibration system for the muon  $g - 2$  experiment”, Nucl. Instrum. Meth. A **842** (2017) 86. doi:10.1016/j.nima.2016.10.047
8. N. Atanov *et al.*, “Energy and time resolution of a LYSO matrix prototype for the Mu2e experiment”, Nucl. Instrum. Meth. A **824** (2016) 684. doi:10.1016/j.nima.2015.09.051
9. N. Atanov *et al.*, “Characterization of a  $5 \times 5$  LYSO Matrix Calorimeter Prototype”, IEEE Trans. Nucl. Sci. **63** (2016) no.2, 596. doi:10.1109/TNS.2016.2522818
10. N. Atanov *et al.*, “Characterization of a prototype for the electromagnetic calorimeter of the Mu2e experiment”, Nuovo Cim. C **39** (2016) no.1, 267. doi:10.1393/ncc/i2016-16267-0
11. N. Atanov *et al.*, “Measurement of time resolution of the Mu2e LYSO calorimeter prototype”, Nucl. Instrum. Meth. A **812** (2016) 104. doi:10.1016/j.nima.2015.12.055
12. G. Pezzullo, “The Mu2e crystal calorimeter and improvements in the  $\mu^-N \rightarrow e^-N$  search sensitivity”, FERMILAB-THESIS-2016-02.
13. F. Iacoangeli *et al.*, “Measurement of the DAFNE Beam Test Facility’s microbunching structure with Micro-Channel Plate based Cherenkov detector”, doi:10.1109/NSSMIC.2014.7431157
14. L. Burmistrov *et al.*, “Test of full size Cherenkov detector for proton Flux Measurements”, Nucl. Instrum. Meth. A **787** (2015) 173. doi:10.1016/j.nima.2014.11.089
15. M. Nishimura *et al.*, “Pixelated Positron Timing Counter with SiPM-readout Scintillator for MEG II experiment”, PoS PhotoDet **2015** (2016) 011.
16. A. M. Baldini *et al.*, “Single-hit resolution measurement with MEG II drift chamber prototypes”, doi:10.1088/1748-0221/11/07/P07011. arXiv:1605.07970 [physics.ins-det].
17. P. W. Cattaneo *et al.*, “Time resolution of time-of-flight detector based on multiple scintillation counters readout by SiPMs”, Nucl. Instrum. Meth. A **828** (2016) 191. doi:10.1016/j.nima.2016.05.038
18. J. Alvarez-Muiz *et al.*, “The AMY experiment: Microwave emission from air shower plasmas”, EPJ Web Conf. **121** (2016) 03010. doi:10.1051/epjconf/201612103010
19. M. Bohacova, “AMY (Air Microwave Yield): Laboratory Measurement of the GHz Emission from Air Showers”, C13-07-02, p.0098
20. S. Anefalos Pereira *et al.*, “Test of the CLAS12 RICH large scale prototype in the direct proximity focusing configuration”, Eur. Phys. J. A **52** (2016) no.2, 23. doi:10.1140/epja/i2016-16023-4
21. G. Croci *et al.*, “GEM-based detectors for thermal and fast neutrons”, Eur. Phys. J. Plus **130** (2015) no.6, 118. doi:10.1140/epjp/i2015-15118-1
22. S. Angius *et al.*, “ICHAOS: A cloud of controls”, Nuovo Cim. C **39** (2016) no.1, 268. doi:10.1393/ncc/i2016-16268-y

23. R. Bedogni *et al.*, “Neutron spectrometry from thermal energies to GeV with single-moderator instruments”, *Eur. Phys. J. Plus* **130** (2015) no.2, 24. doi:10.1140/epjp/i2015-15024-6
24. K. Kittimanapun *et al.*, “SLRI Beam Test Facility Development Project”, doi:10.18429/JACoW-IPAC2016-WEPMY002
25. A. Pichler *et al.*, “Application of photon detectors in the VIP2 experiment to test the Pauli Exclusion Principle”, *J. Phys. Conf. Ser.* **718** (2016) no.5, 052030. doi:10.1088/1742-6596/718/5/052030
26. L. Brianza *et al.*, “Response of microchannel plates to single particles and to electromagnetic showers”, *Nucl. Instrum. Meth. A* **797** (2015) 216. doi:10.1016/j.nima.2015.06.057
27. A. Barnyakov *et al.*, “Beam test results on the detection of single particles and electromagnetic showers with microchannel plates”, 10.1109/NSSMIC.2015.7581993
28. B. Bartoli *et al.*, “The analog Resistive Plate Chamber detector of the ARGO-YBJ experiment”, *Astropart. Phys.* **67** (2015) 47. doi:10.1016/j.astropartphys.2015.01.007
29. B. Bantes *et al.*, “The BGO Calorimeter of BGO-OD Experiment”, *J. Phys. Conf. Ser.* **587** (2015) no.1, 012042. doi:10.1088/1742-6596/587/1/012042
30. M. G. Pelizzo *et al.*, “Optical components in harsh space environment”, *Proc. SPIE 9981, Planetary Defense and Space Environment Applications, 99810G*. doi:10.1117/12.2237966
31. R. de Sangro *et al.*, “Measuring propagation speed of Coulomb fields” *Eur. Phys. J. C* (2015) 75: 137. doi:10.1140/epjc/s10052-015-3355-3

## 8 List of Conference Talks by BTF Authors in 2015-2016

1. P. Valente, “The Frascati LINAC beam facility performance and upgrades”, 38th International Conference on High Energy Physics (ICHEP 2016), Chicago (IL), USA
2. P. Valente, “Status of positron beams for dark photons experiments”, *Advances in Dark Matter and Particle Physics*, 24–27 Oct. 2016, Messina, Italy
3. B. Buonomo, “DAΦNE LINAC: Beam Diagnostics and Outline of the Last Improvements”, 6th International Particle Accelerator Conference (IPAC 2015), Richmond (VA), USA
4. B. Buonomo, “New Gun Implementation and Performance of the DAΦNE LINAC”, 6th International Particle Accelerator Conference (IPAC 2015), Richmond (VA), USA
5. C. Di Giulio, “The Frascati LINAC beam test facility performance and upgrades”, *XV Incontri di Fisica delle Alte Energie (IFAE 2016)*, Genova, Italy.
6. C. Di Giulio, “BTF status and upgrade”, 1st AIDA Annual Meeting, June 14-16, 2016, DESY, Germany.
7. L. Foggetta, “Frascati Beam-Test Facility (BTF) high resolution beam spot diagnostics”, *International Beam Instrumentation Conference (IBIC 2016)*, Barcelona, Spain
8. L. Foggetta, “The Frascati LINAC Beam-Test Facility (BTF) performance and upgrades”, *International Beam Instrumentation Conference (IBIC 2016)*, Barcelona, Spain
9. L. G. Foggetta, “Beam Optimization of the DAΦNE Beam Test Facility”, 6th International Particle Accelerator Conference (IPAC 2015), Richmond (VA), USA

10. L. G. Foggetta, “Evolution of Diagnostics and Services of the DAΦNE Beam Test Facility”, 6th International Particle Accelerator Conference (IPAC 2015), Richmond (VA), USA

## References

1. F. Bossi *et al.*, “What next at LNF: Perspectives of physics research at the Frascati National Laboratories”, INFN-15-05/LNF
2. L. G. Foggetta, B. Buonomo and P. Valente, “Evolution of Diagnostics and Services of the DAΦNE Beam Test Facility”, C15-05-03, p.MOPHA049
3. L. G. Foggetta, B. Buonomo and P. Valente, “Beam Optimization of the DAΦNE Beam Test Facility”, C15-05-03, p.MOPHA048
4. P. Valente *et al.*, “Linear Accelerator Test Facility at LNF: Conceptual Design Report”, arXiv:1603.05651 [physics.acc-ph]
5. B. Buonomo and L. G. Foggetta, “DAΦNE LINAC: Beam Diagnostics and Outline of the Last Improvements”, C15-05-03, p.TUPWA057
6. B. Buonomo, L. G. Foggetta and G. Piermarini, “New Gun Implementation and Performance of the DAΦNE LINAC”, C15-05-03, p.TUPWA056